

SUPPLEMENTARY DATA FOR

Diffusion of organic anions in clay-rich media: effect of porosity exclusion on retardation

R.V.H. Dagnelie^(a,*), S. Rasamimanana^(a), V. Blin^(a), J. Radwan^(a),
E. Thory^(a), J.-C. Robinet^(c), G. Lefèvre^(b)

^(a)DEN-Service d'Etude du Comportement des Radionucléides (SECR),

CEA, Université Paris-Saclay, F-91191 Gif-sur-Yvette, France

^(b) Andra, R&D Division, parc de la Croix Blanche, 92298, Châtenay-Malabry, France

^(c)PSL Research University, Chimie ParisTech-CNRS, Institut de Recherche de Chimie Paris,
11 rue Pierre et Marie Curie, F-75005 Paris, France

* Corresponding author: Romain V.H. Dagnelie, Tel: +33 (0)1 69 08 50 41

Supplementary data

Pages: 10

Tables: 1

Figures: 7

Table S1. Properties of diffusion cell experiments using COx samples and data used to process calculations. [a] Dagnelie et al., 2014 [b] Descostes et al., 2017, [c] this work. *Tracer spiked after a pre-equilibration period with inactive organic molecules (stable species or competitor).

n°/ref	Sample ID	Tracer	A ₀ (MBq)	C ₀ (M)	I.S. (eq.)	Cell	Ø(mm)	L(mm)	V ^{UP} (mL)	V ^{DOWN} (mL)
1 [a]	EST207_16517_2	¹⁴ C-EDTA	0.884	2.70E-02	1.59E-01	static	35.5	10.6	172.8	122.5
2 [a]	EST207_16517_1	¹⁴ C- α -ISA	0.384	2.70E-02	1.59E-01	static	36	10	172.8	122.5
3 [a]	EST207_16517_6	¹⁴ C-Phthalate	0.891	2.70E-02	1.59E-01	static	35.3	11.3	172.8	122.5
4 [a]	EST207_16517	¹⁴ C-Oxalate	0.412	1.00E-03	1.06E-01	static	35	10.9	172.6	122.9
5 [b]	EST207_16517	Eu-EDTA	none	2.70E-02	1.59E-01	static	35.7	9.9	172.5	122
6 [b]	EST207_16517	¹⁵² Eu-EDTA	0.936	2.70E-02	1.59E-01	static	34.8	10.5	172.5	122
7 [c]	EST207_16517	¹⁴ C-Oxalate	0.220	1.00E-06	1.05E-01	static	36	10.5	172.8	122.5
8 [c]	EST207_16517	¹⁴ C-Oxalate*	0.213	1.00E-06	4.05E-01	static	36	10.5	172.8	122.5
9 [c]	EST207_16517	³ H-Phthalate	1.021	1.00E-07	1.05E-01	static	36	10.5	172.8	122.5
10 [c]	EST207_16517	³ H-Phthalate*	1.428	1.00E-07	1.15E-01	static	36	10.5	172.8	122.5
11[c]	EST40471	³ H-Phthalate*	0.653	1.00E-03	1.08E-01	Dynamic	36.04	8.81	149.2	19.9
12 [c]	EST40471	¹⁴ C-Citrate	1.122	1.10E-02	1.16E-01	Dynamic	35.79	8	152.7	19.4
13 [c]	EST40471	¹⁴ C-Citrate*	0.774	9.60E-03	1.15E-01	Dynamic	36.08	9	151	20
14 [c]	EST40471	³ H-Acetate	1.123	1.00E-03	1.06E-01	static	39.5	9.3	172.75	122.6
15 [c]	EST40471	³ H-Adipate	0.961	1.00E-03	1.08E-01	static	39.6	9.7	172.75	122.6

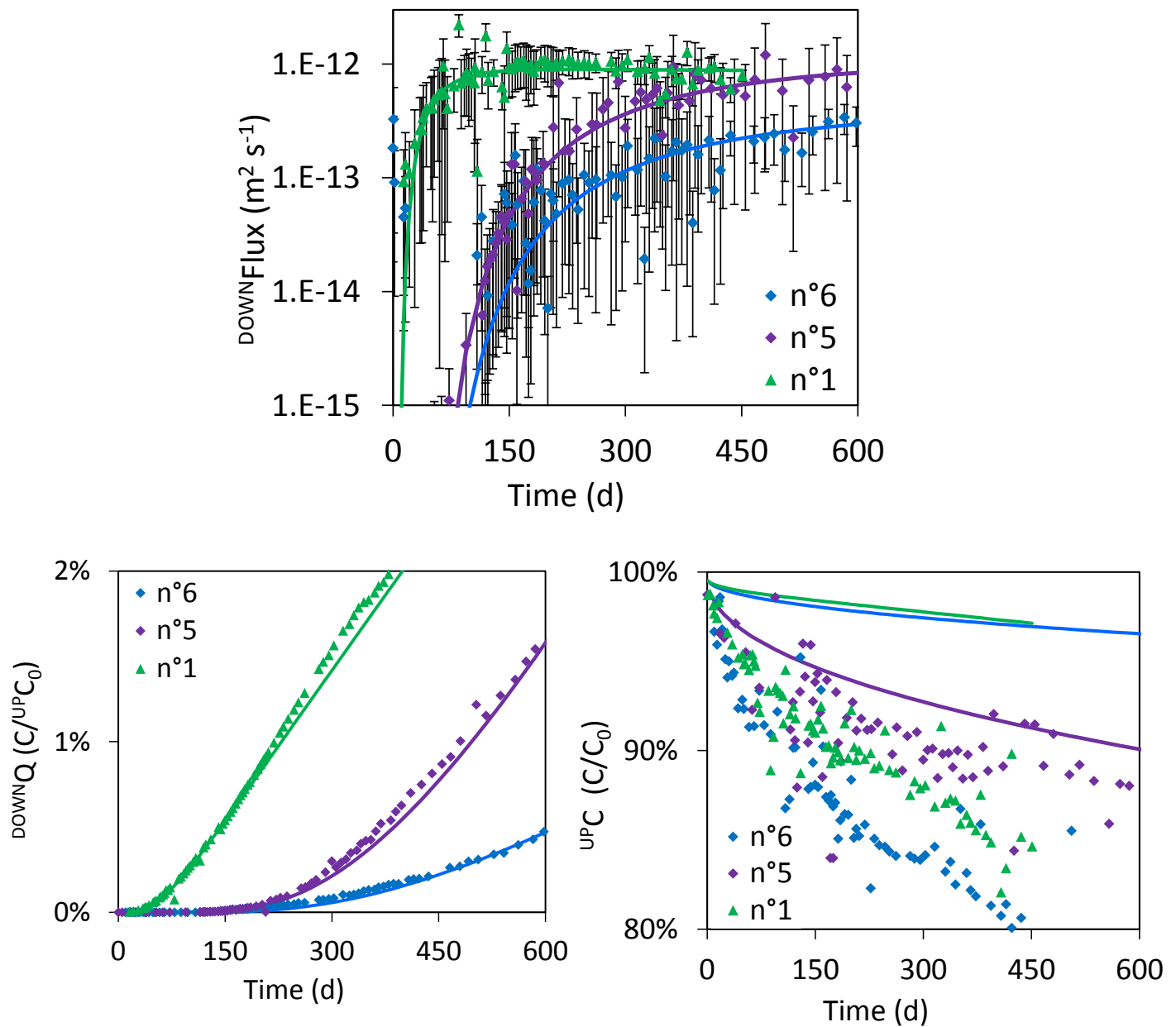


Figure S1: Experimental and modelled data for EDTA species: exp. n°1 (^{14}C -EDTA), exp. n°5 (Eu-EDTA), exp. n°6 (^{152}Eu -EDTA). (Top) Normalized downstream fluxes with uncertainties used for parametric adjustment of the model (solid line). (Bottom) Comparison between experimental data (signs) and modelled data (solid line). (Left) Downstream cumulative concentration (Right) Depletion of upstream concentration. Data of exp. n°1 from (Dagnelie et al., 2014), n°5 and n°6 from Descostes et al. (2017).

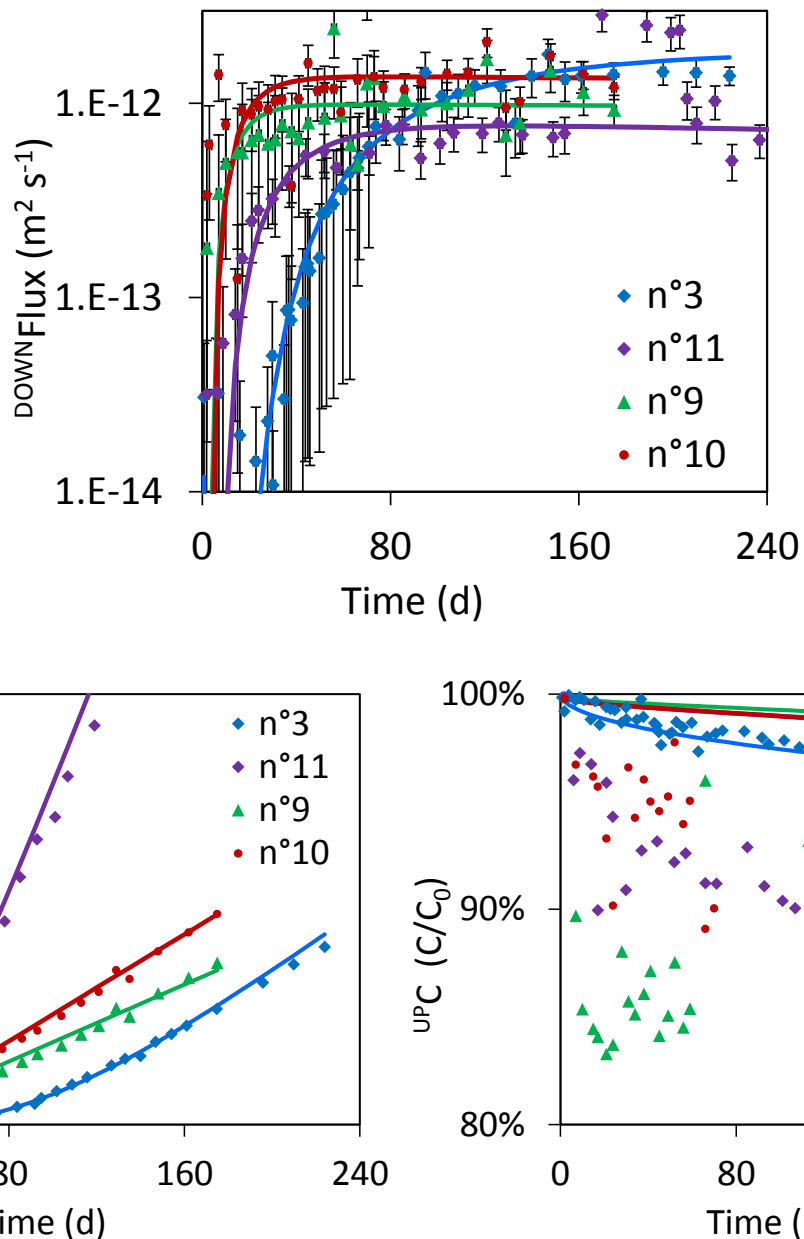


Figure S2: Experimental and modelled data for phthalate species:

exp. n°3 (^{14}C -phthalate without pre-equilibration),

exp. n°11 (^3H -phthalate with pre-equilibration),

exp. n°9 (^3H -phthal. without competing adsorbate),

exp. n°10 (^3H -phthal with 0.1 M competing NaPhthal.)

(Top) Normalized downstream fluxes with uncertainties used for parametric adjustment of the model (solid line). (Bottom) Comparison between experimental data (signs) and modelled data (solid line).

(Left) Downstream cumulative concentration, (Right) Depletion of upstream concentration.

Data of exp. n°3 taken from (Dagnelie et al., 2014).

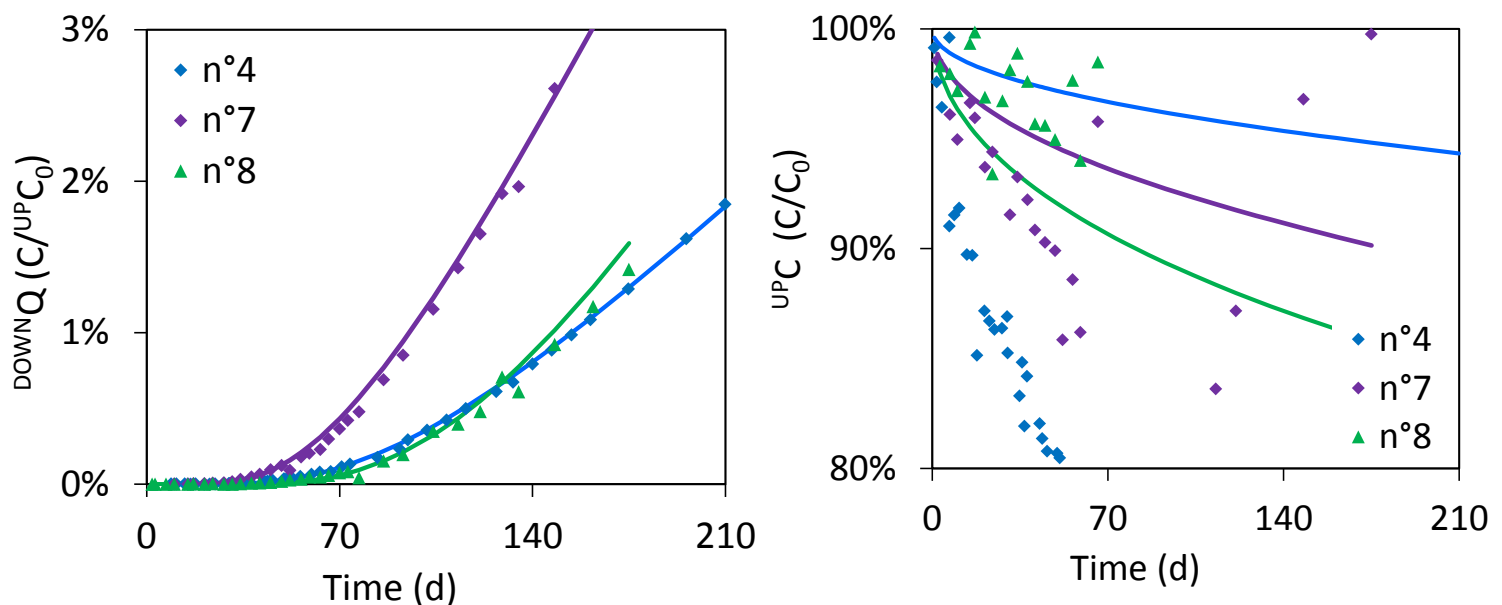
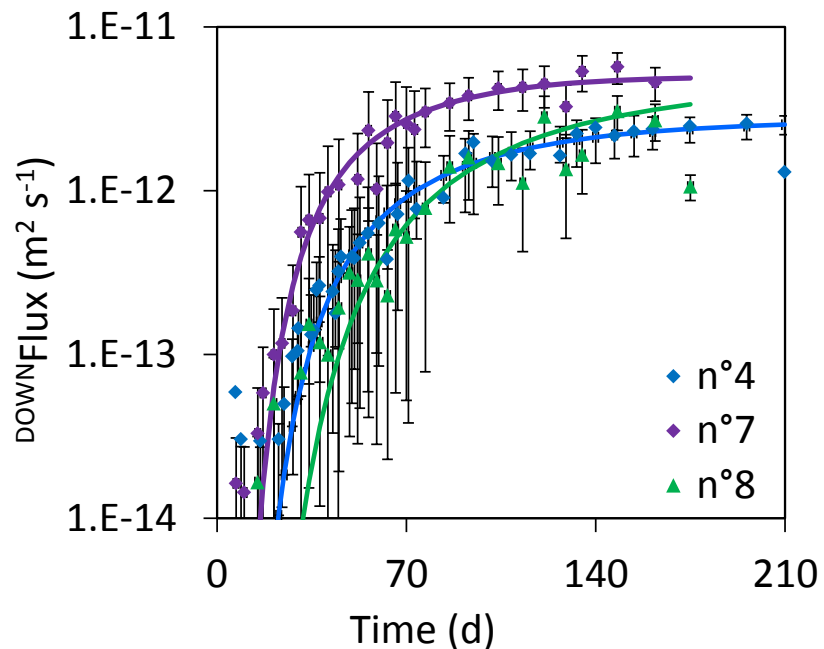


Figure S3: Experimental and modelled data for oxalate species:
exp. n°4 and n°7 (^{14}C -oxalate), exp.n°8 (^{14}C -oxalate with 10 mM competing ISA)

(Top) Normalized downstream fluxes with uncertainties used for parametric adjustment of the model (solid line). (Bottom) Comparison between experimental data (signs) and modelled data (solid line).
(Left) Downstream cumulative concentration, (Right) Depletion of upstream concentration.

Data of exp. n°4 taken from (Dagnelie et al., 2014).

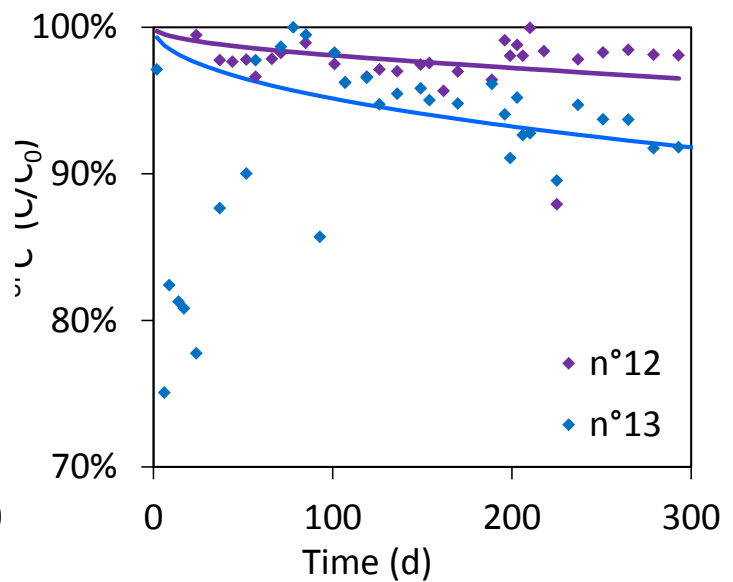
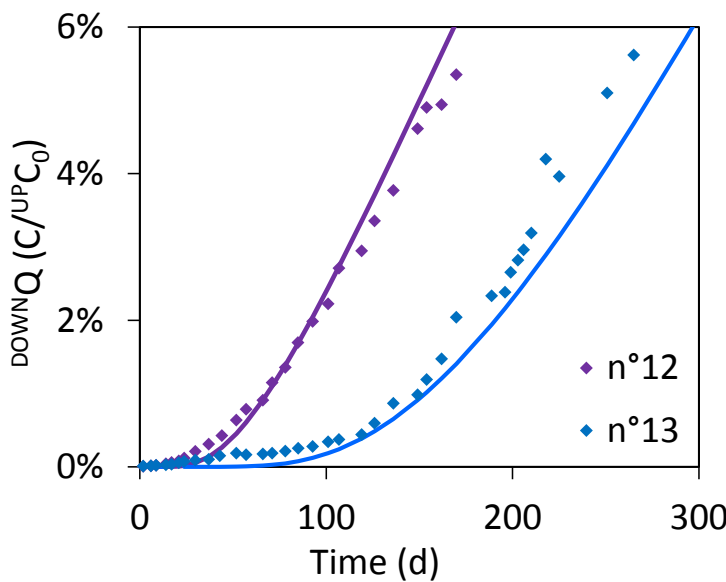
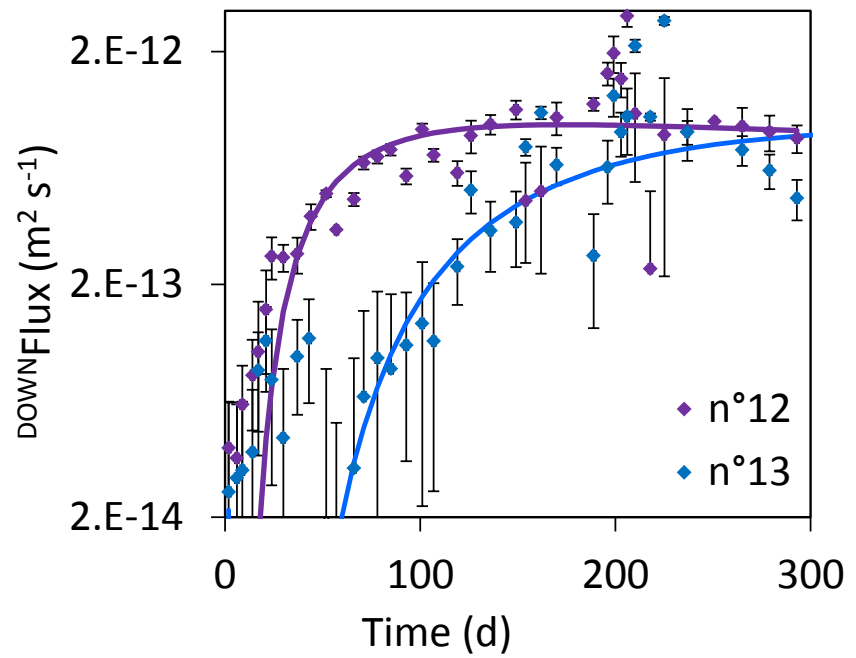


Figure S4: Experimental and modelled data for citrate species:

exp. n°12 (^{14}C -Citrate without pre-equilibration)

exp. n°13 (^{14}C -Citrate with pre-equilibration)

(Top) Normalized downstream fluxes with uncertainties used for parametric adjustment of the model (solid line). (Bottom) Comparison between experimental data (signs) and modelled data (solid line).

(Left) Downstream cumulative concentration, (Right) Depletion of upstream concentration.

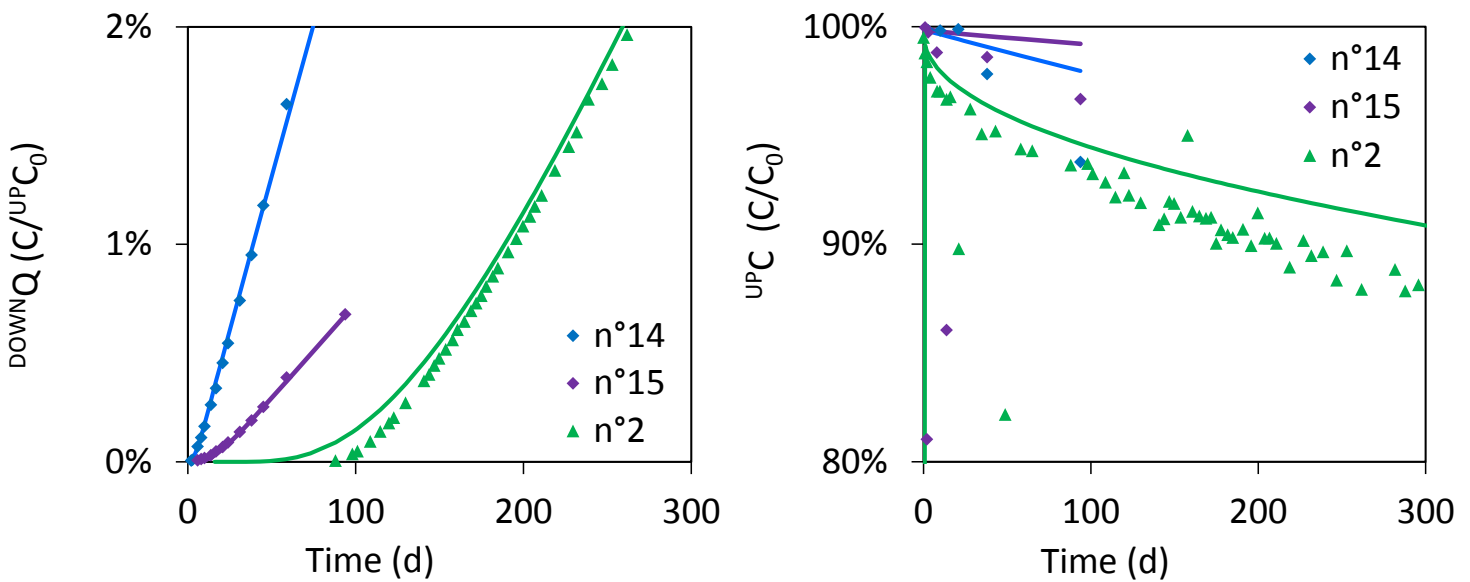
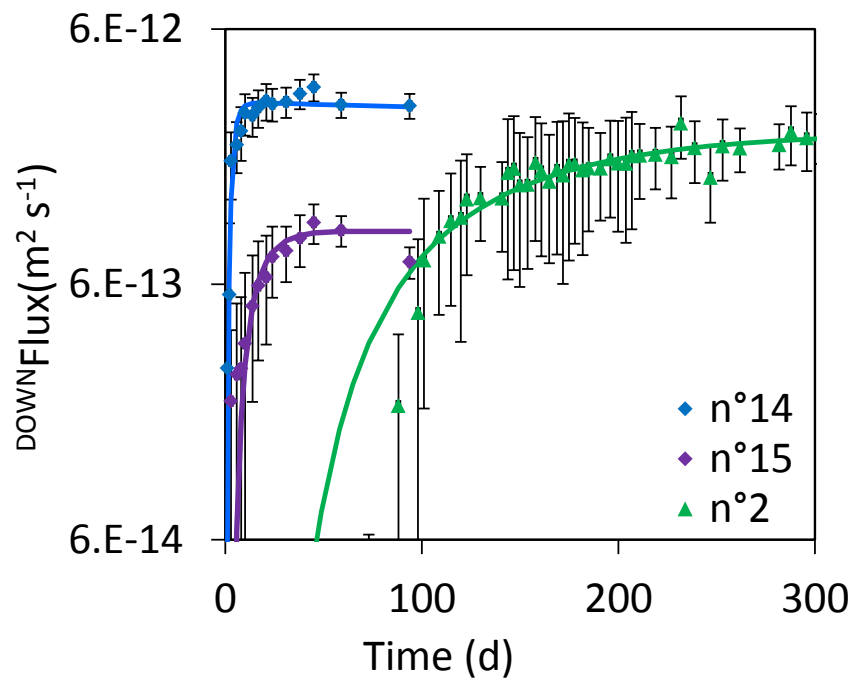


Figure S5: Experimental and modelled data for other species:

exp. n°14 (${}^3\text{H}$ -Acetate), exp. n°15 (${}^3\text{H}$ -Adipate), exp. n°2 (${}^{14}\text{C}$ - α -Isosaccharinate)

(Top) Normalized downstream fluxes with uncertainties used for parametric adjustment of the model (solid line). (Bottom) Comparison between experimental data (signs) and modelled data (solid line).

(Left) Downstream cumulative concentration, (Right) Depletion of upstream concentration.

Data of exp. n°2 taken from (Dagnelie et al., 2014).

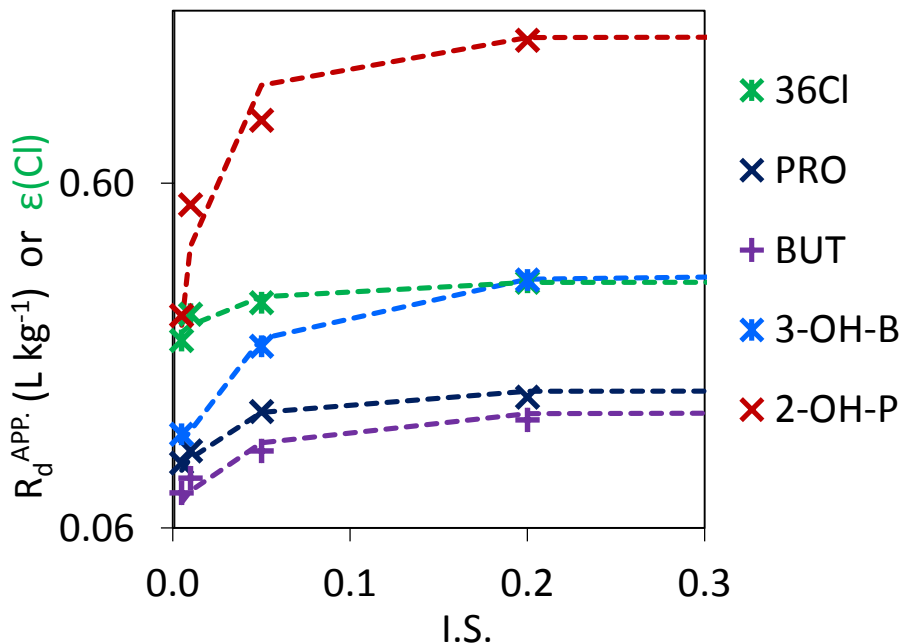


Figure S6: Extrapolation of R_d^{MAX} from $R_d = f(\text{I.S.})$. Crosses: data taken from Chen et al. (2018).
 Solid lines: parametric adjustment made in this study.
 In the case of ^{36}Cl , values stand for anion porosity: $\epsilon(\text{Cl})$.

Table S3. Maximum adsorption measured by percolation of organic anions in compacted illite.
 Data taken from Chen et al. (2018). R_d^{MAX} extrapolated by exponential rise to a plateau (Fig. S6).

Experiment	Organic species	Formula	$R_d^{\text{MAX}} (\text{L kg}^{-1})$
PRO	Propanoate	$\text{C}_2\text{H}_5\text{COO}^-$	0,15
BUT	Butanoate	$\text{C}_3\text{H}_7\text{COO}^-$	0,13
3-OH-B	DL-3-hydroxybutanoate	$\text{CH}_3\text{CH}(\text{OH})\text{CH}_2\text{COO}^-$	0,33
L-2-OH-P	L-2-hydroxypropanoate	$\text{CH}_3\text{CH}(\text{OH})\text{COO}^-$	1,60

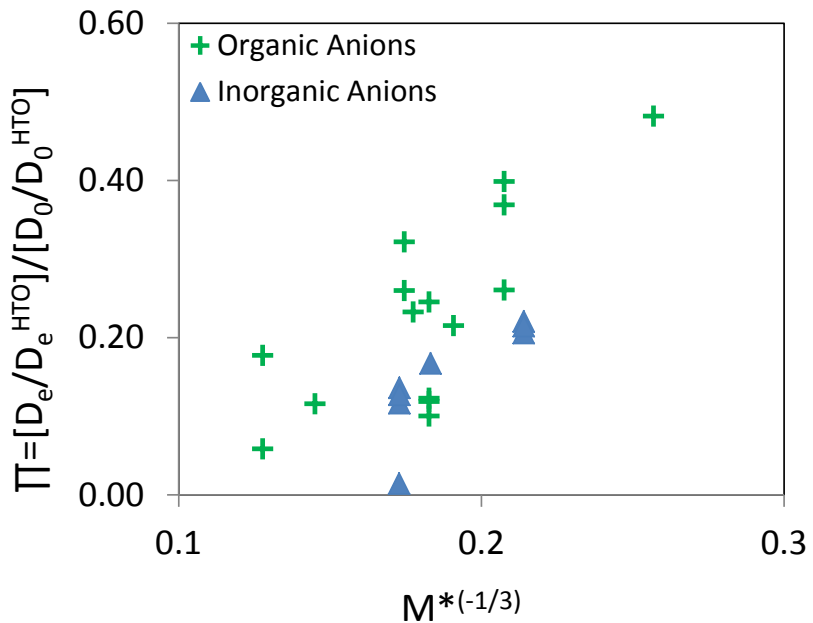


Figure S7: Correlation between Π factor and $M^{-1/3}$. The trend indicates a limited correlation between anion exclusion ($\Pi \ll 1$) and size of molecules (inverse of $M^{-1/3}$). Data on inorganic ions include Cl^- , I^- , SO_4^{2-} , SeO_3^{2-} , NO_3^- diffusion in COx clay rock.

Bibliography:

- Chen, Y., Glaus, M.A., Van Loon, L.R., Mäder, U. 2018. Transport of low molecular weight organic compounds in compacted illite and kaolinite. *Chemosphere* 198, 226-237.
- Dagnelie, R.V.H., Descotes, M., Pointeau, I., Klein, J., Grenut, B., Radwan, J., Lebeau, D., Georgin, D., Giffaut, E., 2014. Sorption and diffusion of organic acids through clayrock: comparison with inorganic anions. *J. Hydrol.* 511, 619-627.
- Descotes, M., Pointeau, I., Radwan, J., Poonoosamy, J., Lacour, J.-L., Menut, D., Vercouter, T., Dagnelie, R.V.H. , 2017. Adsorption and retarded diffusion of Eu^{III} -EDTA⁻ through hard clay rock. *J. Hydrol.* 544, 125-132.
- Gaucher, E., Blanc, P., Bardot, F., Braibant, G., Buschaert, S., Crouzet, C., Gautier, A., Girard, J.-P., Jacquot, E., Lassin, A., Negrel, G., Tournassat, C., Vinsot, A., Altmann, S. (2006) Modelling the porewater chemistry of the Callovo-Oxfordian formation at regional scale. *C.R. Geoscience* **338**, 917-930.
- Jacquier, P., Hainos, D., Robinet, J.-C., Herbette, M., Grenut, B., Bouchet, A., Ferry, C., 2013. The influence of mineral variability of Callovo-Oxfordian clay rocks on radionuclide transfer properties. *Applied Clay Sci.* 83-84, 129-136.

Lerouge, C., Grangeon, S., Gaucher, E.C., Tournassat, C., Agrinier, P., Guerrot, C., Widory, D., Fléhoc, C., Wille, G., Ramboz, C., Vinsot, A., Buschaert, S. (2011) Mineralogical and isotopic record of biotic and abiotic diagenesis of the Callovian–Oxfordian clayey formation of Bure (France). *Geochim. Cosmochim. Acta* **75**, 10, 2633–2663.